Cell Reports
Physical Science

CellPress
OPEN ACCESS

Article

Turning carbon dioxide into dialkyl carbonates through guanidinium-assisted S_N2 ion-pair process

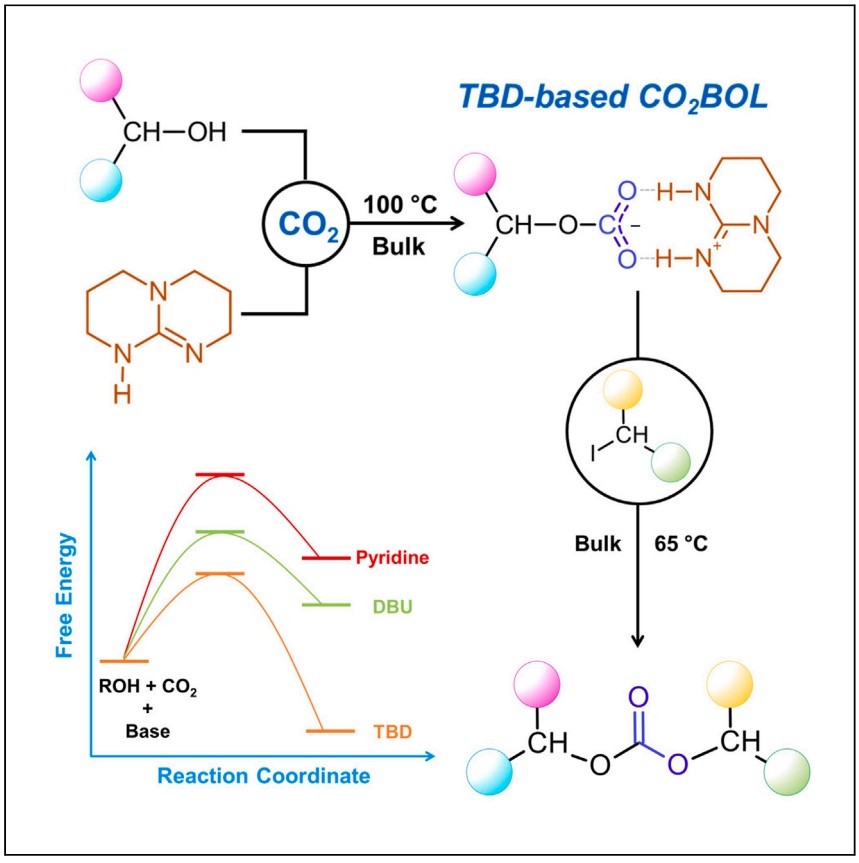

Delcorps et al. demonstrate the superior reactivity of TBD-based carbon dioxide-binding organic liquids in synthesizing linear dialkyl carbonates via a guanidinium-assisted S_N2 ion-pair process. Simulations support this mechanism, and bulk reactions offer practical advantages, enhancing purification and isolation of by-products.

Juliette Delcorps, Kuber Singh Rawat, Mathilde Wells, ..., Pascal Gerbaux, Veronique Van Speybroeck, Olivier Coulembier

olivier.coulembier@umons.ac.be

Highlights

TBD facilitates bulk CO_2 and alcohol binding at 100°C

TBD-based CO_2-binding organic liquids enable synthesis of linear dialkyl carbonates

DFT simulations reveal guanidinium-assisted S_N2 ion-pair process

Noncytotoxicity of residual guanidinium salt suggests pharmaceutical relevance

Delcorps et al., Cell Reports Physical Science 5, 102057
July 17, 2024
https://doi.org/10.1016/j.xcrp.2024.102057

Please cite this article in press as: Delcorps et al., Turning carbon dioxide into dialkyl carbonates through guanidinium-assisted S_N2 ion-pair process, Cell Reports Physical Science (2024), https://doi.org/10.1016/j.xcrp.2024.102057

Cell Reports
Physical Science

CellPress
OPEN ACCESS

Article

Turning carbon dioxide into dialkyl carbonates through guanidinium-assisted S_N2 ion-pair process

Juliette Delcorps,[1] Kuber Singh Rawat,[2] Mathilde Wells,[3] Emna Ben Ayed,[1] Bruno Grignard,[4] Christophe Detrembleur,[5,6] Bertrand Blankert,[3] Pascal Gerbaux,[7] Veronique Van Speybroeck,[2] and Olivier Coulembier[1,8,*]

SUMMARY

The synthesis of dialkyl carbonates, versatile compounds with applications in organic synthesis, pharmaceuticals, and polymers, has attracted considerable attention due to their environmentally benign nature. Here, we describe the selective bimolecular nucleophilic substitution (S_N2) reaction between primary and secondary alkyl iodides with 1,5,7-triazabicyclo[4.4.0]dec-5-ene (TBD)-based carbon dioxide-binding organic liquids. We show that TBD is a great candidate for bulk carbon dioxide and alcohol binding at 100°C. TBD-based carbonate salts are selective for S_N2 processes, allowing them to work with highly reactive alkyl iodide while eliminating unwanted base quaternization either in acetonitrile or in bulk at both 21°C and 65°C. The high reactivity of these TBD-based carbon dioxide-binding organic liquids toward backside S_N2 processes at low temperature is explained by the presence of the TBD.H^+ guanidinium, revealing a unique metal-free cation-assisted S_N2 ion-pair process.

INTRODUCTION

Among the strategies for reducing carbon dioxide (CO_2) emissions, chemical conversion into value-added products has been the spearhead of the research to date.[1–3] From hydrogenation-based to chemical fixation-based products, CO_2 allows for a vast array of valuable chemical compounds to be prepared and designed for specific applications.[4–6] If groundbreaking work on catalyst design now allows for CO_2 to be transformed efficiently, only a few of the technologies available today are economically viable and scalable, such as the production of urea and carbonate-based polymers.[2] Aliphatic polycarbonates are attractive biomaterials owing to the potential CO_2 utilization involved in their production, which is estimated to reach 10–50 Mt/year by 2050.[2] In the current market structure, carbonate-based polymers are mainly prepared by the copolymerization of CO_2 and epoxides.[7] However, they could also be obtained from carbonate-based synthons, either cyclic or linear, themselves potentially derived from CO_2. Since the best strategy for producing polycarbonates—in which carbonate linkages are connected by more than three carbon atoms—is the condensation polymerization of diols and dialkyl carbonates,[8] a high-scale production of the latter is of utmost importance for the plastics industry. In addition to being used as simple intermediates in polymer production, dialkyl carbonates are also important chemical compounds due to their potential use as polar aprotic solvents, monomers for organic glasses-based polymers, synthetic lubricants, plasticizers, intermediates of pharmaceuticals, energy storage enhancers, and CO_2 scavengers.[9–14]

[1]Laboratory of Polymeric and Composite Materials, Center of Innovation and Research in Materials and Polymers, University of Mons, Place du Parc 23, 7000 Mons, Belgium

[2]Center for Molecular Modeling, Ghent University, Technologiepark 46, 9052 Zwijnaarde, Belgium

[3]Laboratory of Pharmaceutical Analysis, Faculty of Medicine and Pharmacy, University of Mons, Place du Parc 23, 7000 Mons, Belgium

[4]FRITCO2T Platform, CESAM Research Unit, University of Liège, Department of Chemistry, Quartier Agora, Sart-Tilman B6A, 4000 Liège, Belgium

[5]Center for Education and Research on Macromolecules (CERM), CESAM Research Unit, University of Liège, Department of Chemistry, Quartier Agora, Sart-Tilman B6A, 4000 Liège, Belgium

[6]WEL Research Institute, Avenue Pasteur 5, 1300 Wavre, Belgium

[7]Organic Synthesis and Mass Spectrometry Laboratory (S2MOs), Materials Institute, University of Mons, Place du Parc 23, 7000 Mons, Belgium

[8]Lead contact

*Correspondence: olivier.coulembier@umons.ac.be

https://doi.org/10.1016/j.xcrp.2024.102057

Please cite this article in press as: Delcorps et al., Turning carbon dioxide into dialkyl carbonates through guanidinium-assisted S_N2 ion-pair process, Cell Reports Physical Science (2024), https://doi.org/10.1016/j.xcrp.2024.102057

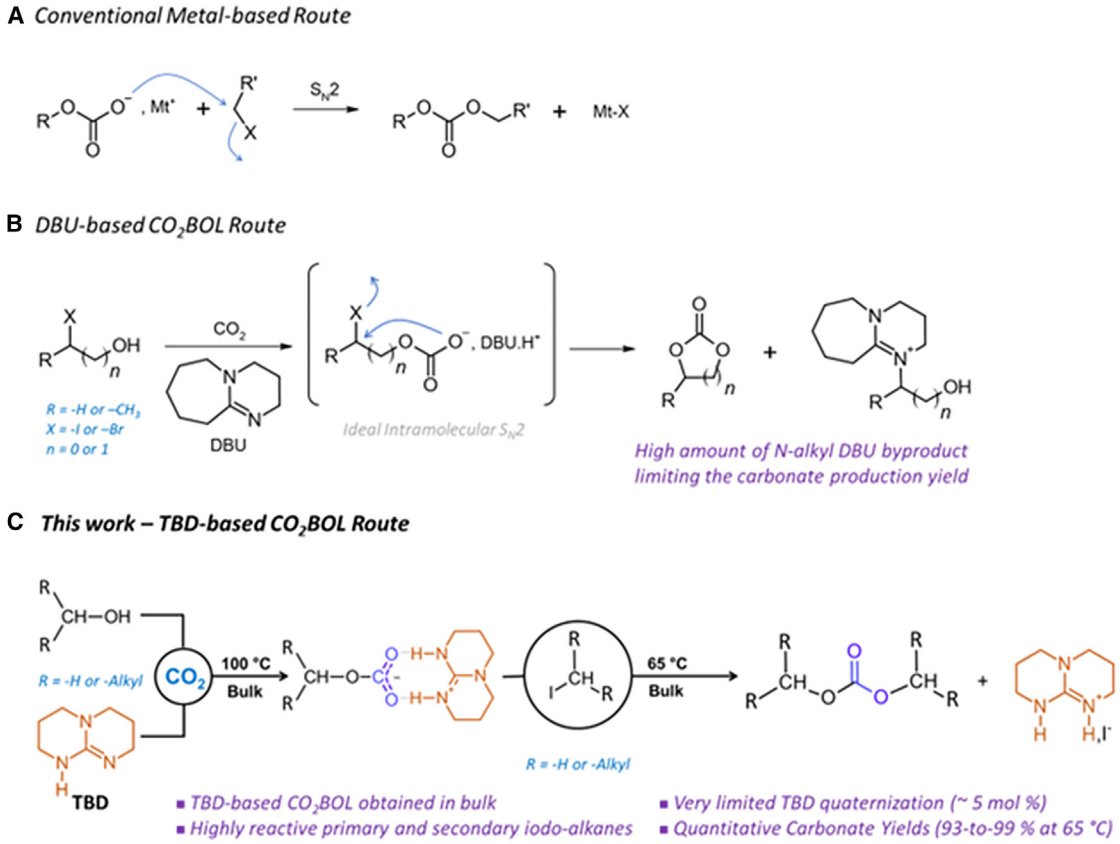

Scheme 1. Preparation of carbonates via S_N2 methods and DBU- and TBD-based CO_2BOL routes

(A) General reaction scheme for the dialkyl carbonate ($ROCO_2CH_2R'$) preparation from an S_N2 reaction between a metal-based carbonate salt ($ROCO_2^-$,Mt^+) and a primary alkyl halide ($R'CH_2X$).

(B) DBU-based CO_2BOL route used for the preparation of ethylene and propylene carbonates.

(C) This work: a TBD-based CO_2BOL route.

Dialkyl carbonates, especially the dimethyl and diethyl forms (DMC and DEC),[15–19] have been commercially synthesized through the phosgene process, Bayer nonphosgene process,[20] ENIChem alcohol oxycarboxylation process,[21] UBE alkyl nitrate carbonylation process,[22] and Asahi-Kasei transesterification process.[15,17,23–25] Although the values of Gibbs free energy indicate that these conventional routes are advantageous,[20] they quickly become unattractive in terms of safety, toxicity, and environment, driving both scientific and industrial interests to CO_2-based processes. In general, there are three main synthetic routes to dialkyl carbonates from CO_2: the direct carboxylation of alcohols, the alcoholysis of urea, and the transesterification of cyclic carbonates with alcohols.[17,26–28] Surprisingly, bimolecular nucleophilic substitution (S_N2) processes between carbonate salts and alkyl halides are not typically used to prepare dialkyl carbonates (Scheme 1A). Although this method offers a simple technological process, the low yield for dialkyl carbonates and rigorous operation conditions generally prevent its popularization. When dialkyl carbonates are prepared from metal-based carbonate salts, the high temperatures adopted to circumvent the poor nucleophilicity of the carbonate active site are generally incompatible with either the carbonate salt's thermal stability or the substrate functionalities. To that end, exotic organic solvents such as *N*-methyl-2-pyrrolidone or *N*,*N*-dimethylacetamide are necessary to maintain the solubility of the metal salts.[28]

Please cite this article in press as: Delcorps et al., Turning carbon dioxide into dialkyl carbonates through guanidinium-assisted S_N2 ion-pair process, Cell Reports Physical Science (2024), https://doi.org/10.1016/j.xcrp.2024.102057

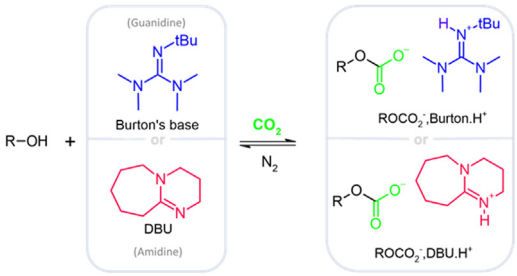

Scheme 2. CO_2BOL synthesis from the DBU amidine base and Burton's guanidine base

Organic compounds such as ionic liquids could moderately improve the S_N2 reaction by enhancing the nucleophilicity of metal-based carbonate salt.[29] As organic molecules offer many advantages over metals, it would be unfortunate to see them as mere additives to metals. To date, only a handful of studies have focused on the preparation of linear dialkyl carbonates using organo-based carbonate salts.[30,31] While Rossi et al. have reported the synthesis of organic carbonates from tetrabutylammonium alkyl carbonates, Bratt and Taylor developed an innovative process based on the use of intermediate methanesulfonyl carbonates. If the latter process suffers from harsh conditions such as high temperatures (>150°C), the former necessitates the synthesis of highly hygroscopic and noncommercially available tetrabutylammonium alkyl carbonates.

Highly interesting for CO_2 capture and sequestration, organic solvent systems known as carbon dioxide-binding organic liquids (CO_2BOLs) have been developed. CO_2BOLs are based on a liquid mixture of an alcohol and amidine or guanidine base, especially 1,8-diazabicyclo[5.4.0]undec-7-ene (DBU) and Burton's base, that chemically binds CO_2 to form amidinium or guanidinium carbonate salts (Scheme 2).[32,33]

In 2019, Khokarale and Mikkola described a one-pot process for the synthesis of 5- and 6-membered cyclic carbonates such as ethylene carbonate (EC) and propylene carbonate (PC) based on the CO_2BOL concept (Scheme 1B).[34] They demonstrated that in presence of the DBU superbase, halohydrins can be effectively converted to cyclic carbonates, except for 2-bromo and 2-iodoethanol, which react equivalently with the amidine and form *N*-alkyl DBU salts. Surprisingly, the authors made no mention of the extremely mild conditions under which the syntheses were carried out, or of the glaring difference in the reactivity of the carbonate salts when they are produced from DBU rather than metals. Although the ease of reaction can obviously be partly explained by the thermodynamic stability of the as-prepared 5- and 6-membered cycles, it is not wrong to envisage that the R-OCO_2^-, DBU.H^+/R'X system also presents similarities to anion-π interactions-based systems[35,36] or to rare ion-pair S_N2 processes,[37–40] in which reaction intermediate and transition state are stabilized (Figure S1).

While guanidines such as 1,1,3,3-tetramethylguanidine (TMG) and Barton's base have already been studied to prepare CO_2BOLs, no one has ever considered the attractive alternative of 1,5,7-triazabicyclo[4.4.0]dec-5-ene (TBD) guanidine. Compared to both TMG and Barton's base, TBD is a unique organic structure due to its high basicity but, more importantly, due to its bifunctionality characterized by two reactive sites at close distance.[41] While its catalytic abilities have already been exploited in various organic reactions, including transesterification,[42,43] transcarbonylation,[44] amidation,[45–53] Michael addition and aldol reactions,[54,55] it also appears as a "magic catalyst" for the polymer community.[56] Ready-to-apply liquid

formulations of TBD are also available, allowing one to overcome the complicated handling of its crystalline delivery form and its rather limited market availability.[41]

Here, we describe the selective S_N2 reaction between primary and secondary alkyl iodides with TBD-based CO_2BOLs (Scheme 1C). By crossing experimental observations and molecular modeling to reveal the most preferred reaction mechanism, we demonstrate that TBD is the most favorable candidate for binding CO_2 and alcohols, especially primary ones. As compared to DBU-based CO_2BOLs, the TBD-based CO_2BOLs are selective to S_N2 processes, allowing us to work with highly reactive alkyl iodides while eliminating undesirable base quaternization. The high reactivity of those TBD-based CO_2BOLs toward backside S_N2 processes is unambiguously explained by the presence of the TBD.H^+ guanidinium revealing a unique metal-free cation S_N2 ion-pair process.

RESULTS AND DISCUSSION

Preparation of TBD-based CO_2BOLs

A fast, selective, and potentially industrially scalable preparation of dialkyl carbonates from a CO_2BOL salt requires adapting to the use of different types of commercially available alkyl halides, especially those bearing excellent leaving groups such as bromide and iodide. Despite iodo-based compounds having been excluded by Khokarale and Mikkola due to their ease of quaternizing DBU during the preparation of EC and PC,[34] we decided to face the challenge by working only with such extremely reactive alkyl halides, thus necessitating the design of a metal-free carbonate salt that is easy to prepare, cheap, and highly selective to a S_N2 process.

The physical and chemical properties of CO_2BOLs can be manipulated by changing alcohol/base pairs. Appropriate organic bases include amidines, guanidines, some amines, and phosphazenes. In comparison to nucleophilic DBU,[57] non-nucleophilic tertiary amines such as triethylamine and Hünig's base seem attractive to get rid of the unwanted *N*-alkylation of the base. However, they have been demonstrated to be ineffective for CO_2BOLs preparation under regular conditions of temperature and pressure.[58] Moreover, phosphazene superbases present some concerns about toxicological issues[59,60] and are not produced on an industrial scale, excluding applications in the chemical industry and, of course, in the present study.

To evaluate the relevance of using TBD to prepare CO_2BOLs from alcohols, we decided to compare its efficiency to the one of the well-known DBU bases. In the presence of DBU, the rate of CO_2 uptake from an alcohol is dependent mainly on the stirring rate of the medium since the reaction is a function of the mass transfer of CO_2 from the gas phase into solution.[32] Under optimal stirring rate conditions, a few seconds are sufficient to almost quantitatively transform a primary alcohol/DBU mixture into a CO_2BOL. To make an efficient comparison between DBU and TBD, we then deliberately decided to work primarily on a static open medium (no stirring rate applied) by simply bubbling CO_2 into the alcohol/base mixture (pCO_2 = 0.2 bar). Conversions were monitored gravimetrically and confirmed from time to time by ^{1}H-NMR spectroscopy. As presented in Figure 1A, such simple experimental modification has a tremendous impact on the overall CO_2 uptake when CO_2BOLs are prepared from different alcohols and the DBU base ($[alcohol]_0/[DBU]_0$ = 1) in bulk (no solvent). While there is a little preference for methanol, ethanol, and 1-propanol over a longer 1-hexanol, these primary alcohols are preferred over secondary alcohols (isopropanol, cyclohexanol, and butan-2-ol)

Please cite this article in press as: Delcorps et al., Turning carbon dioxide into dialkyl carbonates through guanidinium-assisted S_N2 ion-pair process, Cell Reports Physical Science (2024), https://doi.org/10.1016/j.xcrp.2024.102057

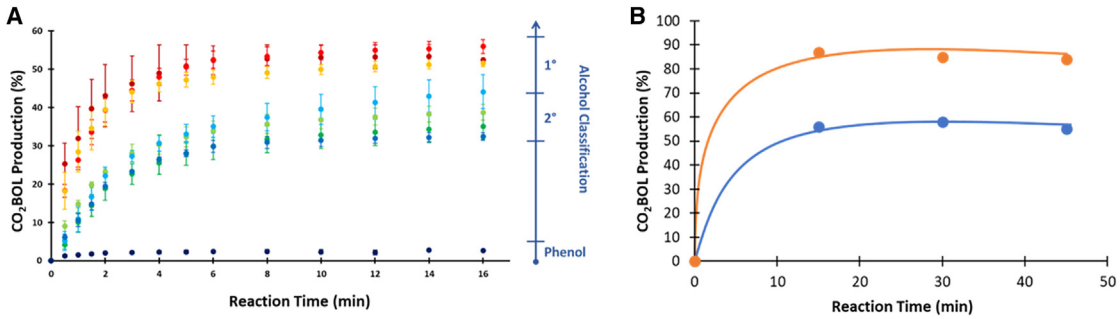

Figure 1. CO_2BOLs production and catalyst comparison

(A) CO_2BOLs production from primary alcohols (maroon dot, methanol, red dot, ethanol, yellow dot, 1-propanol, sky blue dot, 1-hexanol), secondary alcohols (light green dot, isopropanol, green dot, butan-2-ol, medium blue dot, cyclo-hexanol), and phenol (dark blue dot) as activated by DBU ($[alcohol]_0/[DBU]_0 = 1$) at 21°C and under CO_2 bubbling ($pCO_2 = 0.2$ bar). Error bars represent the SDs of 3 trials.

(B) CO_2BOLs production obtained from ethanol as activated by TBD (orange dot) and DBU (blue dot) in MEK ($[ethanol]_0 = [DBU]_0 = [TBD]_0 = 3$ M) at 21°C ($pCO_2 = 0.2$ bar).

and very strongly preferred over the phenol. If such observations appear in line with those of Heldebrant et al.,[32] the maximal CO_2 uptake of this exothermic system (Figure S2), here obtained from primary alcohols, is limited to 52%–56%, reaching a plateau after 5–10 min. Considering those values as reasonable in terms of conversion and kinetics to easily compare the DBU and the TBD bases, we selected those experimental conditions and ethanol as the representative alcohol for our CO_2BOL preparation study with TBD.

Because the semi-crystalline version of TBD has been used, efficiencies of both DBU and TBD bases were experimentally compared by reactions performed in solution for an initial concentration in bases and ethanol of ~3 M. The degree of CO_2 loading in CO_2BOLs is known to control the polarity of the solvent, but conversely the polarity has also been exploited as a means to control CO_2 loading.[61] Since nonpolar solvents aid in the decomplexing of CO_2 from CO_2BOLs, we first decided to compare the respective activities of both DBU and TBD by selecting the polar methyl ethyl ketone (MEK) solvent also known for its great ability to dissolve CO_2 as compared to other solvents such as alcohols.[62]

As expected, the use of TBD considerably increases the overall kinetics of CO_2BOL production and improves the maximal CO_2BOL production value to ~87% (Figure 1B), at least in MEK. By comparing the relative integration of the $CH_3CH_2OCO_2^-$ to the TBD.H^+ methylene signal, the ^{1}H-NMR spectroscopy analysis reveals that the quasi-quantitative CO_2 conversion is attributed to a partial evaporation of the ethanol during the exothermic CO_2BOL formation. Moreover, the oxygen-bound methylene of the ethyl group of the sample shifted from the normal position of ethanol (3.52 ppm in $CDCl_3$) to 3.81 ppm, which is close to the chemical shifts of the DBU-based hexyl carbonate salts (3.90 ppm)[63] or the dihexylcarbonate (4.13 ppm in CCl_4).[64]

To gain further insights into the reaction mechanism and reactivity of both DBU and TBD in the CO_2 conversion toward CO_2BOL, we conducted a detailed investigation using density functional theory (DFT) calculations ($CPCM_{(toluene)}$/ B3LYP-D3(BJ)/6-311^{++}G**,SDD(I) level of theory). Further computational details are given in the experimental procedures section. To better evaluate the relevance of the as-obtained DBU- and TBD-based results, an extra comparison with a nonefficient pyridine base has also been performed (Figure 2).

Please cite this article in press as: Delcorps et al., Turning carbon dioxide into dialkyl carbonates through guanidinium-assisted S_N2 ion-pair process, Cell Reports Physical Science (2024), https://doi.org/10.1016/j.xcrp.2024.102057

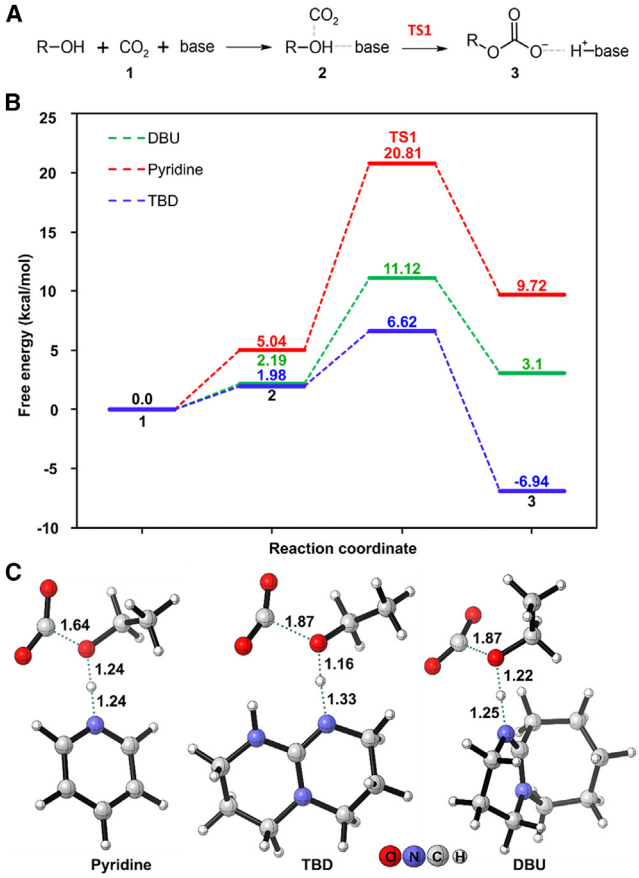

Figure 2. CO_2 activation via ethanol and organic bases: pathways, energy profiles, and transition state geometries

CO_2 activation via ethanol in the presence of bases. (A) Possible reaction pathway and (B) calculated free energy profiles at $CPCM_{(toluene)}$/B3LYP-D3(BJ)/6–$311^{++}G^{**}$ level of theory. (C) Optimized geometries for transition states with bond lengths (in angstroms).
The atom colors are elaborated in the figure (see also Table S1).

The reaction initiates with the interaction between a CO_2 molecule and the base along with ethanol (**1**→**2**). The calculated free energies (ΔG) for this reaction were 5.04, 2.19, and 1.98 kcal/mol (Figure 2B; Table S1) for the pyridine, DBU, and TBD bases, respectively. Next, the transition from intermediate **2** to the final product **3** (**2**→**3**) occurs via a concerted transition state (**TS1**) instead of a stepwise process. Upon closer inspection, it can be observed that in these transition states, the C atom of the CO_2 molecule participates in a reaction with the oxygen atom of ethanol while the base simultaneously abstracts the proton from the alcohol (representative structures are depicted in Figure 2C). The calculated energy barriers ($\Delta G^{\ddagger}$) for pyridine, DBU, and TBD were determined to be 15.77, 8.93, and 4.64 kcal/mol, respectively. These results are in agreement with our experiments and indicate that TBD is the most favorable candidate for this reaction compared to the other two bases, and, most importantly, DBU. Moreover, the overall reaction free energy profile also reveals a strong interaction between the carbonate anion and $TBD.H^+$, leading to an overall exothermic reaction-free energy of −6.94 kcal/mol compared to the endothermicity observed for $DBU.H^+$ (3.1 kcal/mol) and $pyridine.H^+$ (9.72 kcal/mol). The CO_2 activation using the base only was also explored in previous reports,[65,66] and we found that in this scenario as well, activation by TBD (2.89 kcal/mol) requires

a lower energy barrier compared to DBU (6.56 kcal/mol) (Figure S18). These barriers are lower compared to the CO_2 activation by ethanol in the presence of bases. Nevertheless, the final products are found to be 5.09 and 5.81 kcal/mol more favorable for TBD and DBU, respectively, when CO_2 reacts with ethanol rather than with base alone.

To demonstrate that the preparation of CO_2BOLs from TBD is a promising and efficient process, the ability of the guanidine base to quantitatively convert longer primary alcohols into carbonate salts has been investigated by adjusting the experimental conditions to improve the CO_2BOL conversion. Long primary alcohols do not solubilize the semi-crystalline version of TBD at room temperature (RT), thus requiring one to either use an efficient solvent to solubilize reactants while stabilizing the as-produced carbonate salt or to generate CO_2BOLs in the melt state. To the best of our knowledge, the second strategy has never been studied and could represent a real breakthrough for the industrial production of CO_2BOLs. 1-Heptanol has been used as a representative candidate for the rest of our study.

In 2008, Jessop et al. briefly stated that the production of CO_2BOLs from DBU and alcohols proceeds to great conversion in $CDCl_3$.[63] To get rid of the relatively slow kinetics observed under static conditions, 1-heptanol and TBD were therefore solubilized in this solvent ($[1\text{-heptanol}]_0 = 4$ M, $[OH]_0/[TBD]_0 = 1$) and subjected to a CO_2 bubbling treatment ($pCO_2 = 0.2$ bar, 2–3 bubbles per second) under a high stirring rate (~500 rpm).[32] Under these experimental conditions, our ^{1}H-NMR data show that the reaction proceeds to very high conversions. Specifically, the proton assignable to the OH function of the 1-heptanol initially shifts downfield and then completely disappears after 10 min of reaction. Concomitantly, the N-H signal of the TBD shifts downfield by +0.53 ppm to the benefit of the guanidium protons signal (Figure S3). By comparing integration values before and after reaction, a conversion of 95% $\pm$ 5% is calculated. Considering the moderate accuracy of the ^{1}H-NMR integration, such a result indicates either a complete or an almost-complete conversion to the alkyl carbonate salt.

To complement our observation and clearly visualize the important role of the chloroform solvent, the CO_2 activation was also evaluated when the carbonate salt is produced under $CHCl_3$ solvation. Appropriate DFT calculations were then investigated and compared to a representative toluene-based medium (Figure S4). The calculated energy barriers (**TS1**) for DBU and TBD in $CHCl_3$ were found to be 7.15 and 3.99 kcal/mol, respectively. These energy barriers were 1.78 and 0.65 kcal/mol lower compared to the toluene solvent for DBU and TBD, respectively (Figure S19). Furthermore, the comprehensive analysis of the free energy profile of the reaction indicated that the final product (**3**) is favored more when $CHCl_3$ is the solvent, with an additional free energy stabilization of 2.93 and 2.08 kcal/mol for DBU and TBD, respectively. Moreover, TBD exhibited a more favorable reaction free energy (−9.02 kcal/mol) when compared to DBU (0.17 kcal/mol). This observation aligns well with the experimental results, suggesting that TBD is a better base for CO_2 activation compared to DBU, especially in $CHCl_3$. Additionally, we performed a comparative analysis of various solvents in the activation of CO_2 using TBD. Our computational findings, as illustrated in Figure S19, indicate that acetonitrile (ACN) leads to a greater thermodynamic stability compared to toluene and $CHCl_3$.

Although academically very interesting, producing CO_2BOLs in organic solvents presents certain disadvantages. Generally speaking, in the limited context of a single production of CO_2BOLs, the use of solvent considerably reduces any interest in

Please cite this article in press as: Delcorps et al., Turning carbon dioxide into dialkyl carbonates through guanidinium-assisted S_N2 ion-pair process, Cell Reports Physical Science (2024), https://doi.org/10.1016/j.xcrp.2024.102057

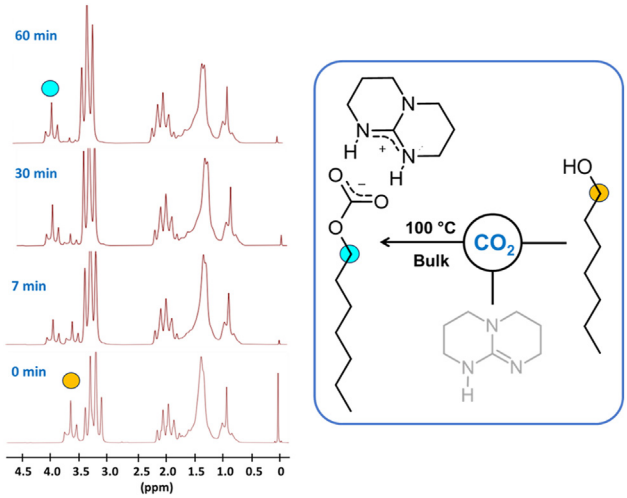

Figure 3. Bulk production of CO_2BOLs via heat-activated TBD and 1-heptanol mixture under CO_2 exposure

^{1}H-NMR spectra (between δ = 0 ppm and δ = 4.5 ppm) of an equimolar mixture of 1-heptanol and TBD during a CO_2 treatment at 100°C (see also Figure S6).

industrial production. In the more specific context of our study, and in view of the DFT results presented above, chloroform contributes considerably to the general stabilization of CO_2BOLs, limiting *de facto* their reactivity toward the alkyl halides used to prepare dialkyl carbonates through a one-pot S_N2 reaction. To get rid of such a problem, we investigated the possibility of producing CO_2BOLs at a temperature sufficiently high to solubilize TBD into the alcohol without using any solvent.

As already stated, liquid long primary alcohols such as 1-heptanol do not solubilize the semi-crystalline version of TBD at 21°C. When heated at 100°C for few seconds, the two-phase mixture turns into a clear fluid solution. By cooling down the medium to RT, the TBD starts to recrystallize producing the heterogeneous 1-heptanol/guanidine mixture. To produce the corresponding CO_2BOL in bulk, the equimolar mixture of 1-heptanol and TBD was therefore heated up and subjected to a CO_2 exposure (pCO_2 = 0.2 bar) under a high stirring rate (~500 rpm) at a constant temperature of 100°C. Although slower than that in $CHCl_3$ solution, treating the homogeneous mixture at 100°C under a CO_2 atmosphere enables the corresponding carbonate salt to be produced selectively in a near-quantitative yield (~96%), after 1 h of reaction and without the use of solvent (Figures 3 and S6). Obviously, the working temperature must be sufficiently high but also below the decomposition temperature of the CO_2BOL to prevent the potential thermal release of CO_2 from the TBD-based salt, a topic slated for further investigation. However, the liberation of CO_2 from the CO_2BOL suggests a potential avenue for recyclability. Indeed, examination of the TBD-based salt's thermal stability revealed that under a nitrogen flow (pN_2 = 0.2 bar), it takes 1.5 h to achieve ~90% degradation at 90°C, whereas complete degradation occurs within 0.5 h at 110°C (Figure S5). Subsequent to thermal degradation, the alcohol and TBD are recovered (Figure S7). Consequently, the CO_2BOL could be readily regenerated by reintroducing CO_2 into the mixture.

Preparation of linear dialkyl carbonates from TBD-based CO_2BOLs

Taking into account the experimental data in the literature on reactions involving the use of DBU-based carbonate salts and alkyl halides, it would appear that, leaving aside the poisoning alkylation reactions of DBU, the production of carbonates is

Table 1. Reaction yields

		Bulk			ACN	
Alkyl iodine	Entry	Yield (%) at 21°C	Yield (%) at 65°C	Entry	Yield (%) at 21°C	Yield (%) at 65°C
Iodoethane	1	~99	~99	4	93	~99
1-Iodooctane	2	23	~99	5	67	93
2-Iodopropane	3	67	96	6	97	95

Yields of heptyl-OCO_2^-, TBD.H^+ salt with different alkyl iodides as reacted in bulk and ACN (2 M) at 21°C and 65°C. Yields are determined by ^{1}H-NMR analysis from the crude mixture taking into account the engaged TBD-based salt content.

somehow based on a S_N mechanism. The primary nature of the alkyl halides generally used seems to support the fact that the mechanism involved implies an S_N2 process. Despite this, the generally mild experimental conditions, compared to those adopted for the use of metal-based carbonate salts, make the exact nature of this process unclear. This is all the more true as the nucleophilic nature of carbonate salts is supposed to be very weak, making the process theoretically fastidious. To remove the doubt and define this reaction as accurately as possible, a series of experimental carbonatations were carried out and supplemented by DFT theoretical calculations.

Various linear dialkyl carbonate syntheses were performed by adding primary and secondary alkyl iodides to a heptyl-OCO_2^-,TBD.H^+ salt, pregenerated by the treatment of an equimolar mixture of 1-heptanol and TBD under CO_2 bubbling for 1.5 h at 100°C (conversion ~95%). Iodoethane and 1-iodooctane were selected as primary alkyl iodides, while 2-iodopropane was used as a representative secondary alkyl halide. Reactions were performed for 24 h under air by using 1 equiv of alkyl iodide as compared to the initial 1-heptanol. Since all of the reactants are liquid, nucleophilic substitution reactions were performed in ACN (2 M) but also in bulk at 21°C and 65°C (Table 1). Carrying out S_N reactions without solvent should favor the formation of the expected solid TBD.H^+, I^- salt by-product, simplifying the separation process and easily enhancing reaction purity.

Carrying out the carbonatation reactions in ACN gives high yields whatever the temperature and the nature of the alkyl iodide (Table 1, entries 4–6). This observation certainly highlights a reaction mechanism based on an S_N2 process. Since the frontside pathway is highly disfavored because of the increased steric repulsion resulting from the proximity of the carbonate nucleophile and I^- leaving group in the transition state, the hypothesis of an S_N2 backside process appears more convincing. It is interesting to note that the overall polarity of the solvent is not crucial since high yields of reactions are also obtained in bulk, especially at 65°C (Table 1, entries 1–3). More interestingly, it is worth noting that the yields observed when iodoethane is used as the alkyl iodide are somehow identical with or without ACN (Table 1, entries 1 and 4). Although results obtained when using 1-iodooctane must be discarded due to a partial crystallization of the carbonate produced in bulk at 21°C (Table 1, entry 2), the use of 2-iodopropane also provides highly acceptable results in the absence of solvent at RT, considering the secondary nature of this alkyl iodide (Table 1, entry 3). Based on the concept of ion pairs introduced and developed by Winstein et al.,[67] all of these observations suggest that the hypothetical backside S_N2 process does not proceed from free ions or solvent-separated ions but from contact ion pairs where the countercation (i.e., the TBD.H^+ guanidinium) and the anion (i.e., the heptyl-OCO_2^- carbonate anion) are in close proximity to each other.

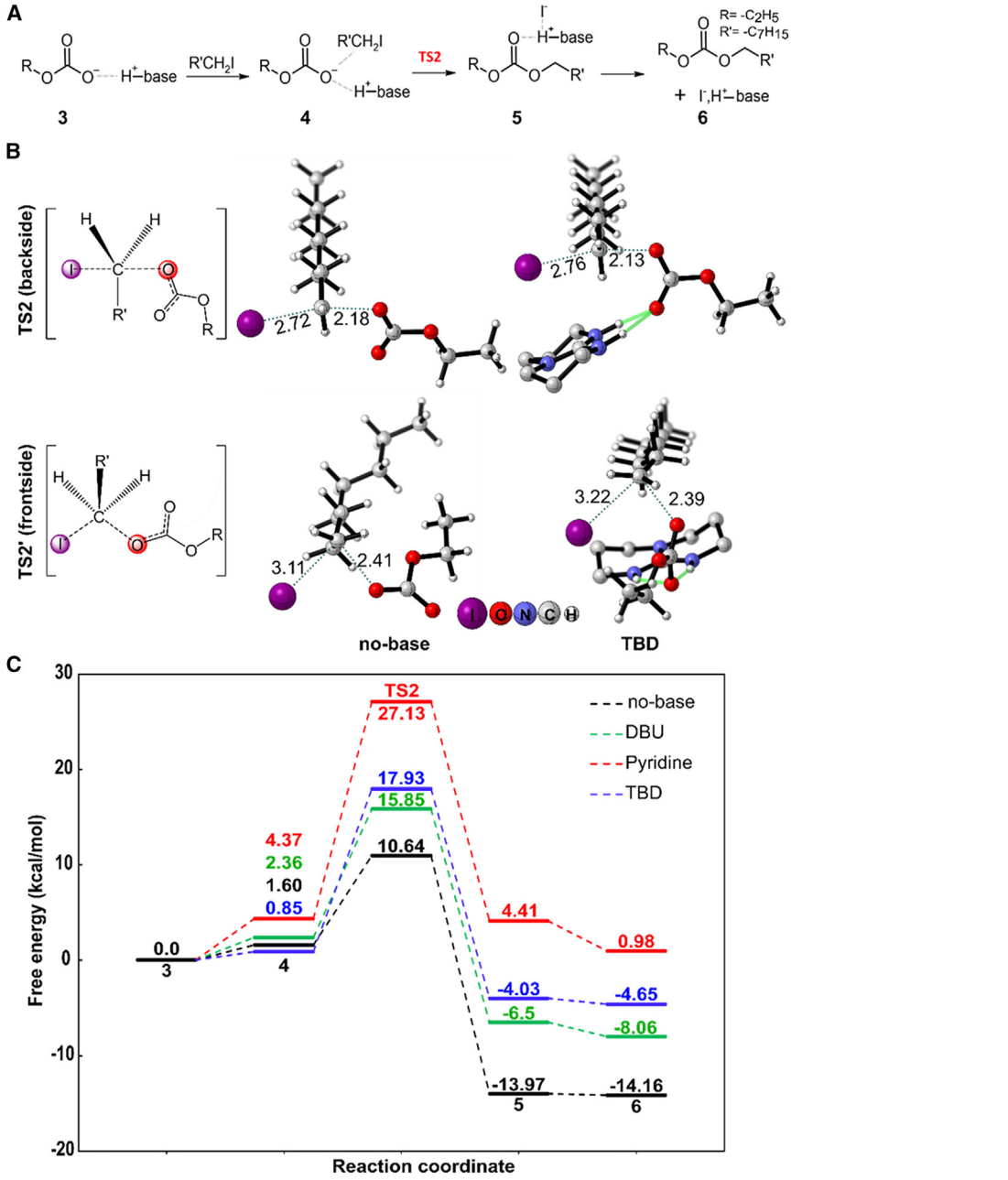

Figure 4. DFT mechanistic investigation of TBD-based CO_2BOL reactivity toward alkyl iodides: comparison with and without DBU and pyridine

S_N2 reaction mechanism: (A) possible reaction pathway, (B) optimized geometries for transition states (bond lengths in angstroms), and (C) calculated free energy profile (backside attack) at $CPCM_{(toluene)}$/B3LYP-D3(BJ)/6–$311^{++}G^{**}$, SDD(I) level of theory.

H atoms are omitted from TBD for clarity. The atom colors are elaborated in the figure (see also Figure S20; Table S2).

To understand the high reactivity of the TBD-based CO_2BOLs in regard to the alkyl iodides and to shed some light on the mechanism involved, mechanistic investigations at the DFT level were performed. To make an accurate comparison, the reactivity of TBD-based CO_2BOLs has been compared to the ones hypothetically obtained from both DBU and pyridine bases. Simulations were performed by considering intermediate **3** (Figure 2A) and 1-iodooctane. The proposed reaction pathway is illustrated in Figure 4A. Two scenarios have been hypothesized, one in

which the mechanism implies a carbonate anion in absence of its TBD.H^+ countercation (labeled "no-base") and another in the presence of the protonated base cation (labeled "pyridine," "DBU," and "TBD"). In each scenario, the S_N2 reaction was examined via two distinct transition states (Figure 4B): (1) the carbonate anion attacks via the backside (**TS2**) of the leaving group (I^-) or (2) the carbonate anion attacks from the frontside of the leaving group (**TS2′**). Based on the calculated free energy barriers (Figures 4C and S20; Table S2), it is evident that the backside attack is more favorable in all of the cases. Interestingly, a backside attack without TBD.H^+ shows the most favorable path, with a free energy barrier of 9.04 kcal/mol, which is 28.03 kcal/mol lower compared to when the carbonate anion approaches from the frontside (Table S2). However, the calculated barriers via **TS2** are 13.48, 17.08, and 22.76 kcal/mol for DBU, TBD, and pyridine, respectively. This indicates that, compared to an amidinium cation, the involvement of a guanidinium cation demands a higher barrier to accomplish the process. The reason stems from the disruption of the strong interaction between the cation and the carbonate anion during the substitution process. As a result, the separation of the carbonate anion and base.H^+ in intermediate **3** requires large free energies of 44.23 and 38.22 kcal/mol (Figure S21) for TBD and DBU, respectively. Such high energy barriers confirm that free ions are not involved and that contact ion pairs are acting as nucleophiles in the S_N2 process. Nevertheless, noncovalent interaction (NCI) analysis[68] reveals that the energy required to break the interaction can be counterbalanced by stabilizing both the leaving and attacking groups through the formation of NCIs with TBD.H^+ in **TS2**. To investigate the role of these interactions, various configurations of **TS2** (Figure 5) were computed by altering the manner in which TBD.H^+ interacts with the leaving I^- ion and attacking carbonate anion groups. When both I^- and the unreactive O atom of the carbonate anion engage in interactions with TBD.H^+ (I···TBD and N–H···O), a barrier of 17.08 kcal/mol is required (Figure 5A). As clearly represented by Figure 5E, such an optimized transition state induces an attractive NCI between the TBD.H^+ and the leaving I^-, strongly supporting a guanidinium-assisted S_N2 ion-pair process. Any alteration in these interactions (Figures 5F–5H) leads to a higher barrier.

Overall, as compared to DBU and pyridine, the presence of TBD is quite crucial to assist in the CO_2 activation and subsequent S_N2 reaction with alkyl iodides through a unique guanidinium-assisted S_N2 ion-pair process. Additionally, a combined free energy profile for the reaction gives additional support to the role of different bases (Figure 6).

We also explored the free energy profile using ACN, toluene, and $CHCl_3$ solvents for the TBD base (Figure S22). A comprehensive analysis of the overall reaction free energy profile shows a preference for ACN, showcasing energy advantages of 6.99 and 2.85 kcal/mol over toluene and $CHCl_3$, respectively. This observation aligns well with our experimental results, demonstrating that ACN exhibits improved catalytic performance compared to the bulk.

Considering the reactants involved, performing reactions in bulk presents an interesting asset—the precipitation of the TBD.H^+, I^- salt and its simple isolation from the crude medium. Whatever the alkyl iodide used, and after only a few minutes, a significant amount of a white compound indeed starts to precipitate, making its isolation by filtration easy. While the ^{1}H-NMR analysis of that compound confirms the presence of a protonated guanidinium (TBD.H^+) (Figure S15), the presence of an iodide counteranion has been unambiguously certified by electrospray ionization mass spectrometry analysis (ESI-MS) (Figure S16). Indeed, besides ions

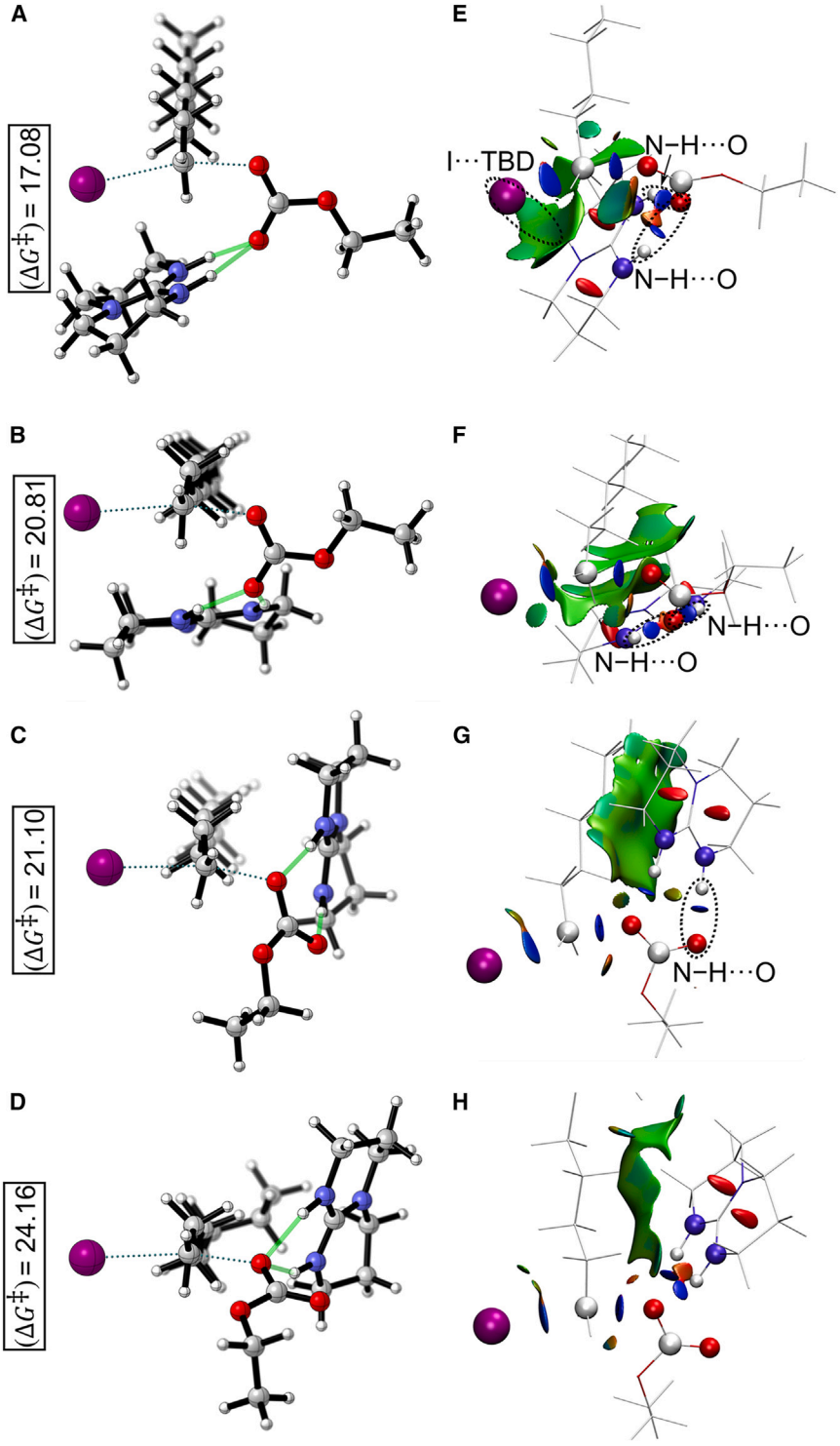

Figure 5. Transition state geometries and NCI analysis of TBD-based S_N2 reaction: Impact of NCIs on energy barriers

(A–D) Optimized geometries for transition states (TS2) involving TBD base in backside-attack S_N2 reaction, considering various NCIs between TBD.H^+ and both leaving I^- and the attacking carbonate anion groups.

(E–H) The calculated energy barriers (in kilocalories per mole) are presented alongside their corresponding NCI plots, providing a detailed visualization of the impact of these interactions on the energy barriers. Isosurface colors reflect the nature and strength of the interactions, with blue indicating regions of strong attractive interactions, green representing areas of attractive interactions, and red highlighting regions of repulsion.

Please cite this article in press as: Delcorps et al., Turning carbon dioxide into dialkyl carbonates through guanidinium-assisted S_N2 ion-pair process, Cell Reports Physical Science (2024), https://doi.org/10.1016/j.xcrp.2024.102057

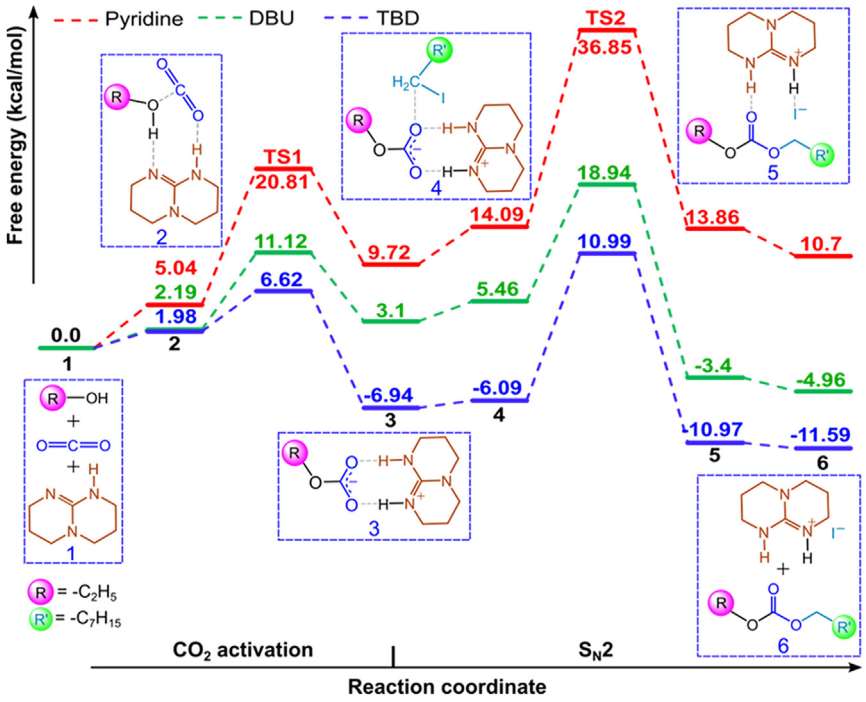

Figure 6. Role of TBD in CO_2 activation and S_N2 reaction: Comparative free energy profile with DBU and pyridine

A combined free energy profile for CO_2 activation and S_N2 ion-pair reaction using different bases calculated at $CPCM_{(toluene)}$/B3LYP-D3(BJ)/6–$311^{++}G^{**}$, SDD(I) level of theory. The reactants, products, and intermediates of TBD are enclosed in blue dashed-line boxes.

corresponding to the cationic part of organic salts, such as ionic liquids, aggregate ions associating the parent ion with one or more ionic liquid molecules are often detected upon ESI in the positive ion mode,[69] making the identification of both the cationic and anionic parts of an organic salt possible in a single MS analysis. In Figure S16, besides the dominant signals at *m/z* 140.1 and 279.2 that are readily ascribed to $[TBD+H]^+$ and $[2TBD+H]^+$ ions, the singly charged ions detected at *m/z* 407.1 correspond to such an aggregate associating two protonated TBD molecules to a single iodide anion, typically $[2TBD+2H+I]^+$, whose detection supports our first hypothesis. Satellite signals at *m/z* 168.1, 196.2, and 435.2 are also detected and attest to the presence of TBD molecules that have been quaternized by iodoethane. In our opinion, the detection of these signals is attributable to the presence of at least 5 mol % of $TBD^+C_2H_5$. Such *N*-quaternized TBD comes from the fact that iodoethane has been used in slight excess as compared to the heptyl-OCO_2^-, $TBD.H^+$ salt initially produced at ~95 mol % from the 1-heptanol ($[iodoethane]_0 = [TBD]_0 = [1\text{-heptanol}]_0 \sim (100/95).[\text{heptyl-}OCO_2^-, TBD.H^+]$).

All of the linear dialkyl carbonates have been characterized by ^{1}H-NMR spectroscopy and gas chromatography (GC)-MS analysis (Figures S8, S9, and S11–S14). Figure 7 is a representative example of carbonate obtained in bulk at 21°C after filtration of the $TBD.H^+$, I^- by-product (Table 1, entry 1). GC-MS analyses have been performed under chemical ionization (CI) conditions using methane as the CI gas, since under electron ionization conditions no molecular ions were detected. Under $CI(CH_4)$, the C_7H_{15}-O-C(=O)-O-C_2H_5 carbonate is detected as protonated molecules, $[M + H]^+$, at *m/z* 189.2. Note that the adduct ions at *m/z* 217.2 and 229.2 are generated in the ionization source running at high pressure in methane. Besides the quasi-molecular ions, the fragment ions detected at *m/z* 91.0, 119.1, and 131.1 arise from a 98-u (atomic mass unit) loss (C_7H_{14}) from the *m/z* 189.2, 217.2, and 229.2

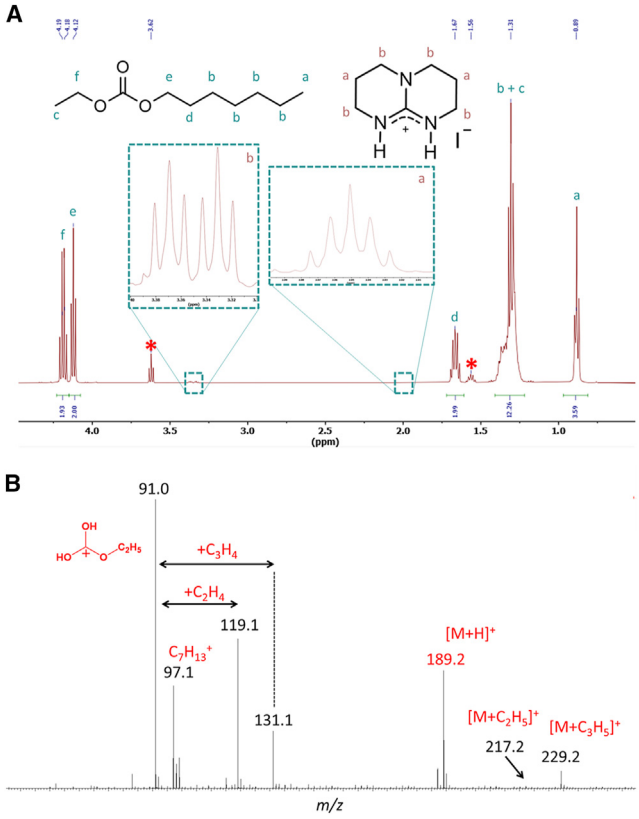

Figure 7. Characterization of heptyl-ethyl carbonate by ^{1}H-NMR and GC-MS analysis

(A) ^{1}H-NMR ($CDCl_3$, 500 MHz) of the heptyl-ethyl carbonate (see Table 1, entry 1) between δ = 0.5 and 4.5 ppm (with asterisk signals belonging to the residual 1-heptanol) and (B) its corresponding GC-MS analysis (CI (CH_4) HRMS (high-resolution mass spectrometry) $C_{10}H_{21}O_3$ $[M + H]^+$ m/z_{exp} = 189.1517, m/z_{th} = 189.1491; Δ = 2.6 mDa). m/z_{exp}, experimental mass-to-charge ratio; m/z_{th}, thereotical mass-to-charge ratio.

parent ions, respectively. We further confirm the elemental composition of the *m/z* 189.2 ions as $[C_{10}H_{20}O_3+H]$ using an accurate mass measurement (high-resolution MS [HRMS]) experiment, confirming the presence of the C_7H_{15}-O-C(=O)-O-C_2H_5 composition. This last sample was finally analyzed by Fourier transform infrared spectroscopy (FTIR), along with both 1-heptanol and the heptyl-OCO_2^-,TBD.H^+ CO_2BOL salt (Figure S10). By comparing spectra, distinctive changes are clearly visible, constituting reliable evidence for the formation of the dialkyl carbonate function, supporting *de facto* the S_N2 ion-pair process. Before reacting with 1-iodoethane, the CO_2BOL exhibits a C=N ring stretching vibration at 1,570 cm^{-1} and N–H stretching at 3,152 and 3,232 cm^{-1}, confirming the presence of the protonated TBD. This is consistent with the ^{1}H-NMR data. Additionally, the strong absorption at 1,655 cm^{-1} and the weak peak at 1,388 cm^{-1} correspond to the stretching vibrations of C=O and C–O– groups of the carbonate anion, respectively. In comparison, the IR spectrum of the C_7H_{15}–O–C(=O)–O–C_2H_5 dialkyl carbonate shows a distinctive absorption at 1,744 cm^{-1}, attributed to the asymmetric stretching vibration of the C=O group, and a band at ~1,251 cm^{-1}, corresponding to the symmetric stretching vibration of the C–O–C linkage within the carbonate group.

While the nature of the isolated TBD.H^+, I^- salt might suggest a possible reconversion as solar cell components or as catalysts for the fixation of CO_2 to epoxides,[70–72]

Please cite this article in press as: Delcorps et al., Turning carbon dioxide into dialkyl carbonates through guanidinium-assisted S_N2 ion-pair process, Cell Reports Physical Science (2024), https://doi.org/10.1016/j.xcrp.2024.102057

whatever the linear dialkyl carbonate produced in bulk, the residual presence of the guanidinium salt (<1 mol % based on ^{1}H-NMR analysis) was always pointed out (Figure 7A, insets between δ = 3.3 and 3.4 ppm and between δ = 2.0 and 2.1 ppm). To avoid a tedious extraction process involving the use of a large quantity of organic solvent, we reasoned that the salt could be considered an acceptable contaminant regarding the final application of the as-produced carbonate. Because linear dialkyl carbonates represent an important intermediate class of pharmaceuticals, a salt toxicity test has been undertaken. The study was performed on fetal human epithelial cells FHs74Int (American Type Culture Collection [ATCC], CCL-241). Cells were incubated at 37°C for 24 h before being treated with a series of 2-fold dilutions of the TBD.H$^+$, I$^-$ salt. The effective tested concentrations ranged from 0.78 to 200 μM. After 24 h, cell viability was assessed through a [3(-(4,5-dimethylthiazol-2-yl)-2,5-diphenyltetrazolium bromide)] (MTT) assay.[73] Cell viability (%) was calculated compared to a negative control. Within the tested concentration range, the TBD.H$^+$, I$^-$ salt displayed no significant toxicity on FHs74Int cells (Figure S17). The slope of the curve was shown to be nonsignificantly different from zero following a Fisher-Snedecor test (p = 0.7151). This wide interval of concentrations was chosen as it is presumed to be far above the likely residual levels of the catalyst. FHs74Int cells were selected as they are derived from nonpathological human intestinal tissue and constitute a good model to study the toxicity of any compound/food that could come into contact with the intestinal epithelial barrier.[74] Although these preliminary results are promising, other cell lines could also be investigated in the future, notably liver-derived cells to evaluate the effect of a potential metabolization on the cytotoxicity of TBD.H$^+$, I$^-$.

We compared the formation of DBU- and TBD-based CO_2BOLs both experimentally and theoretically, and concluded that TBD is a better candidate for the formation of CO_2BOLs. We also demonstrated the ability of TBD to form CO_2BOLs in bulk with quasi-quantitative yields. This allowed us to attempt an S_N2 on the as-prepared CO_2BOLs using various alkyl iodides without performing any prior purification. Experiments and DFT calculations showed that despite a significant energy barrier, the reaction still proceeded without much difficulty. TBD-based carbonate salts exhibited remarkable selectivity for S_N2 processes, consistently achieving yields above 90% across a range of conditions in both acetonitrile and bulk settings at temperatures from 21°C to 65°C. This underscores the robustness and versatility of TBD-based carbonate salts in promoting S_N2 reactions with highly reactive alkyl iodides. The high reactivity of these TBD-based CO_2BOLs toward backside S_N2 processes at low temperatures is explained by the presence of the TBD.H$^+$ guanidinium, revealing a unique metal-free cation-assisted S_N2 ion-pair process. By performing reactions in bulk, the TBD.H$^+$, I$^-$ by-product crashes out and is easily filtered out. In the pharmaceutical use of dialkylated carbonates, the presence, even residual, of the guanidinium salt does not likely pose a problem in view of its noncytotoxicity, at least on FHs74Int cells.

EXPERIMENTAL PROCEDURES

Resource availability

Lead contact

Further information and requests for resources and reagents should be directed to and will be fulfilled by the lead contact, Olivier Coulembier (olivier.coulembier@umons.ac.be).

Materials availability

This study did not generate new unique reagents.

Data and code availability

All of the processed data are available in the paper or supplemental information. Further questions will be addressed by the lead contact upon reasonable request.

Materials

Carbon dioxide N50 (≥99.999%) was supplied by Air Liquide. 1-Propanol (≥99%), 2-butanol (99%), 1-hexanol (anhydrous, ≥99%), deuterated chloroform (0.03 vol % tetramethylsilane, deuteration degree minimum 99.8% for NMR spectroscopy, stabilized with Ag), as well as 1-heptanol were purchased from Sigma-Aldrich. Methanol (GPR Rectapur) and propan-2-ol were purchased from VWR. Iodoethane (≥98%, stabilized with Cu) and 1-iodooctane were acquired from Alfa Aesar. Cyclohexanol (99%) and DBU (≥98%) were supplied by Thermo Scientific. Phenol (≥99%, for biochemistry, loose crystals) and 2-butanone (or MEK, ACS Reagent) were acquired from Acros Organics. Ethanol (denaturated with 3% diethyl ether, Desinfectol) was purchased from Chemlab. TBD was supplied by Apollo Scientific. 2-Iodopropane (stabilized with Cu chip) was purchased from TCI. All of the reagents were used as received.

NMR spectroscopy

CO_2 conversion kinetics were followed time-to-time through ^{1}H-NMR using a Spinsolve 60 Ultrabenchtop NMR spectrometer (Magritek). All of the spectra were acquired according to the following parameters: aq = 6.4 s, repetition time = 10 s, pulse angle = 90, and ns = 32.

Final dialkyl carbonate products were characterized by ^{1}H-NMR using a Bruker AVANCEII 500 MHz apparatus at RT in chloroform-d_1 ($CDCl_3$). All of the spectra were acquired according to the following parameters: aq = 6.8 s, d1 = 10 s, sw = 12, o1p = 5, ns = 32 (1,024 for ^{13}C).

FTIR

FTIR was performed to further demonstrate the formation of both the heptyl-OCO_2^-,TBD.H^+ salt and the ethyl-heptyl carbonate using a Bruker Tensor 27 spectrometer.

DFT calculations

All of the calculations were performed using the DFT as implemented in Gaussian 16 package[75] with Becke's three-parameter hybrid exchange and Lee-Yang-Parr's correlation functional (B3LYP).[76,77] A mixed basis set of SDD for the I atom and the 6-311^{++}G** basis set for all of the other atoms were considered.[78–80] To account for the solvent effect of toluene, a conductor-like polarizable continuum model (CPCM) was applied.[81] Chloroform and acetonitrile solvents were also considered for comparison. All of the structures were optimized using Grimme's dispersion correction D3(BJ) to consider noncovalent interactions.[82,83] Confirmation of intermediates and transition states was achieved through harmonic vibrational frequencies, ensuring the absence of imaginary frequencies for intermediates and the presence of one imaginary frequency for transition states corresponding to the desired transformation. Free energies and free energy barriers were calculated at 298.15 K and 1-atm pressure. The NCI plot was used and depicted with visual molecular dynamics to gain more insight into the crucial noncovalent interactions between base and reactants in the transition state.[68,84] All of the optimized structures were illustrated using the visualization package CYLView.[85]

Cytotoxicity tests

Fetal human epithelial cells FHs74Int (ATCC, CCL-241) were cultivated and seeded in 96-well plates (2×10^4 cells per well). Cells were incubated at 37°C for 24 h before being treated with a series of 2-fold dilutions of the TBD.H^+, I^- salt. Culture medium (Hybri-Care medium [ATCC] supplemented with 10% fetal bovine serum) was used for the dilutions, and the effective tested concentrations ranged from 0.78 to 200 μM. After 24 h, cell viability was assessed through an MTT assay, a colorimetric test that allows the measurement of cellular metabolic activity. Briefly, the cell medium was discarded and replaced by 200 μL MTT solution at 0.5 mg/mL in PBS. Following a 4-h incubation period, the MTT solution was removed from the plates, and DMSO was added to dissolve the formed formazan crystals. The absorbance was measured at 570 nm using a SpectraMax M2 (Molecular Devices). Cell viability (%) was calculated compared to a negative control (untreated cells in presence of culture medium).

General procedure for the synthesis of DBU-based CO_2BOLs

A vial equipped with a septum is charged with DBU (3 mL, 0.0201 mol) and an alcohol (0.0201 mol). Two needles (20G), one of which is connected to the CO_2 tank, are then used to pierce the septum and bubble carbon dioxide (pCO_2 = 0.2 bar) onto the reaction mixture. The reaction is performed at RT and kinetically studied by gravimetry or ^{1}H-NMR (60 MHz).

General procedure for the synthesis of TBD-based CO_2BOLs in MEK

A vial equipped with a septum is charged with TBD (2.7979 g, 0.0201 mol), ethanol (1.170 mL, 0.0201 mol), and MEK (6.7 mL, C_{TBD} = 3 M). Two needles (20G), one of which is connected to the CO_2 tank, are then used to pierce the septum and bubble carbon dioxide (pCO_2 = 0.2 bar) onto the reaction mixture. The reaction is performed at RT and kinetically studied by gravimetry or ^{1}H-NMR (60 MHz).

General procedure for the synthesis of TBD-based CO_2BOLs from 1-heptanol

A vial equipped with a septum and a stir bar is charged with a mixture of TBD (2.7979 g, 0.0201 mol) and 1-heptanol (2.8414 mL, 0.0201 mol) in $CDCl_3$ (5 mL, C_{TBD} = 4 M) or in bulk. Two needles (20G), one of which is connected to the CO_2 tank, are then used to pierce the septum and bubble carbon dioxide (pCO_2 = 0.2 bar) onto the reaction mixture. The reaction is performed at RT (in $CDCl_3$) or at 100°C (in bulk) and under 500 rpm stirring. Reaction kinetics were studied by ^{1}H-NMR spectroscopy. ^{1}H-NMR (500 MHz, $CDCl_3$): δ = 3.90 (t, 2H), 3.30 (dt, 8H), 2.00 (quint, 4H), 1.60 (quint, 2H), 1.30 (m, 8H), and 0.87 (t, 3H).

General procedure for the alkylation of CO_2BOLs

Alkylation reactions were performed on CO_2BOLs obtained according to the procedure described in the previous section. No treatments or purifications were performed on the reaction mixtures. Selected alkyl iodides (0.0201 mol) were added to the vial after the completion of the synthesis of the CO_2BOLs. Reactions were performed at RT or 65°C, in bulk or in ACN (2M), and under 500 rpm stirring for 24 h. Reaction kinetics were studied by ^{1}H-NMR spectroscopy.

(1) Ethyl-heptyl carbonate: ^{1}H-NMR (500 MHz, $CDCl_3$): δ = 4.18 (q, 2H), 4.12 (t, 2H), 1.67 (quint, 2H), 1.31 (t, 8H), 0.89 (t, 3H). GC-MS: CI (CH_4) HRMS $C_{10}H_{21}O_3$ $[M + H]^+$ m/z_{exp} = 189.1517, m/z_{th} = 189.1491; Δ = 2.6 mDa.
(2) Octyl-heptyl carbonate: ^{1}H-NMR (500 MHz, $CDCl_3$): δ = 4.12 (t, 4H), 1.66 (quint, 4H), 1.30 (b.s., 18H), 0.89 (t, 6H). GC-MS: CI (CH_4) HRMS $C_{16}H_{33}O_3$ $[M + H]^+$ m/z_{exp} = 273.2432, m/z_{th} = 273.2430; Δ = 0.2 mDa.

(3) isoPropyl-heptyl carbonate: ^{1}H-NMR (500 MHz, $CDCl_3$): δ = 4.87 (m, 1H), 4.12 (t, 2H), 1.66 (quint, 4H), 1.29 (d, 14H), 0.88 (t, 3H). GC-MS: CI (CH_4) HRMS $C_{11}H_{23}O_3$ $[M + H]^+$ m/z_{exp} = 203.1644, m/z_{th} = 203.1647; Δ = −0.3 mDa.

(4) TBD.H$^+$, I$^-$: ^{1}H-NMR (500 MHz, $CDCl_3$): δ = 3.35 (d.t., 8H), 2.03 (quint, 4H). MS: ESI HRMS $C_{14}H_{28}N_6I$ [2 $TBDH^+$ + I^-] m/z_{exp} = 407.1413, m/z_{th} = 407.1420; Δ = −0.7 mDa.

SUPPLEMENTAL INFORMATION

Supplemental information can be found online at https://doi.org/10.1016/j.xcrp.2024.102057.

ACKNOWLEDGMENTS

J.D. and E.B.A. acknowledge the support of the AXA Research Fund for the funding of this project. O.C. acknowledges support for his position as a senior research associate for the F.R.S.-FNRS of Belgium and AXA Professor in Chemistry. K.S.R. and V.V.S. acknowledge the research board of UGent (Bijzonder Onderzoeksfonds) through a Concerted Research Action (GOA010-17). The computational resources and services (Stevin Supercomputer Infrastructure) were provided by the VSC (Flemish Supercomputer Center), funded by UGent, Research Foundation Flanders, and the Flemish Government-department EWI. C.D. is the FNRS Research Director and thanks FNRS for financial support.

AUTHOR CONTRIBUTIONS

Conceptualization: O.C.; methodology: J.D., K.S.R., B.G., and C.D.; software: K.S.R.; validation: J.D., E.B.A., M.W., C.D., and P.G.; investigation: J.D., E.B.A., K.S.R., B.G., and M.W.; writing – original draft: J.D. and K.S.R.; writing – review & editing: O.C., J.D., K.S.R., E.B.A., B.G., C.D., B.B., P.G., and V.V.S.; visualization: J.D., K.S.R., E.B.A., and O.C.; supervision: O.C., C.D., P.G., B.B., and V.V.S.

DECLARATION OF INTERESTS

The authors declare no competing interests.

Received: March 12, 2024
Revised: April 23, 2024
Accepted: May 25, 2024
Published: June 17, 2024

REFERENCES

1. Aresta, M., Dibenedetto, A., and Angelini, A. (2014). Catalysis for the Valorization of Exhaust Carbon: From CO_2 to Chemicals, Materials, and Fuels. Technological Use of CO_2. Chem. Rev. *114*, 1709–1742. https://doi.org/10.1021/cr4002758.

2. Hepburn, C., Adlen, E., Beddington, J., Carter, E.A., Fuss, S., Mac Dowell, N., Minx, J.C., Smith, P., and Williams, C.K. (2019). The Technological and Economic Prospects for CO_2 Utilization and Removal. Nature *575*, 87–97. https://doi.org/10.1038/s41586-019-1681-6.

3. Liu, Y., and Lu, X.-B. (2023). Current Challenges and Perspectives in CO_2 - Based Polymers. Macromolecules *56*, 1759–1777. https://doi.org/10.1021/acs.macromol.2c02483.

4. Li, Y.-N., He, L.-N., Diao, Z.-F., and Yang, Z.-Z. (2014). Carbon Capture with Simultaneous Activation and Its Subsequent Transformation. In Advances in Inorganic Chemistry, *66*Advances in Inorganic Chemistry (Elsevier), pp. 289–345. https://doi.org/10.1016/B978-0-12-420221-4.00009-3.

5. Centi, G., and Signori, F. (2014). Green Carbon Dioxide: Advances in CO_2 Utilization (Wiley)).

6. Hu, B., and Suib, S.L. (2014). Synthesis of Useful Compounds from CO_2. In Green Carbon Dioxide, G. Centi and S. Perathoner, eds. (Wiley), pp. 51–97. https://doi.org/10.1002/9781118831922.ch3.

7. Wei, P., Bhat, G.A., and Darensbourg, D.J. (2023). Enabling New Approaches: Recent Advances in Processing Aliphatic Polycarbonate-Based Materials. Angew. Chem. Int. Ed. *62*, e202307507. https://doi.org/10.1002/anie.202307507.

8. Park, J.H., Jeon, J.Y., Lee, J.J., Jang, Y., Varghese, J.K., and Lee, B.Y. (2013). Preparation of High-Molecular-Weight Aliphatic Polycarbonates by Condensation Polymerization of Diols and Dimethyl Carbonate. Macromolecules *46*, 3301–3308. https://doi.org/10.1021/ma400360w.

9. Schäffner, B., Schäffner, F., Verevkin, S.P., and Börner, A. (2010). Organic Carbonates as Solvents in Synthesis and Catalysis. Chem. Rev. *110*, 4554–4581. https://doi.org/10.1021/cr900393d.

10. Gryglewicz, S., Oko, F.A., and Gryglewicz, G. (2003). Synthesis of Modern Synthetic Oils

Based on Dialkyl Carbonates. Ind. Eng. Chem. Res. *42*, 5007–5010. https://doi.org/10.1021/ie030322m.

11. Ono, Y. (1997). Catalysis in the Production and Reactions of Dimethyl Carbonate, an Environmentally Benign Building Block. Appl. Catal. Gen. *155*, 133–166. https://doi.org/10.1016/S0926-860X(96)00402-4.

12. Chaban, V.V., and Andreeva, N.A. (2022). Dialkyl Carbonates Enforce Energy Storage as New Dielectric Liquids. J. Mol. Liq. *367*, 120454. https://doi.org/10.1016/j.molliq.2022.120454.

13. Chaban, V.V., Andreeva, N.A., Bernard, F.L., M Dos Santos, L., and Einloft, S. (2023). Chemical similarity of dialkyl carbonates and carbon dioxide opens an avenue for novel greenhouse gas scavengers: cheap recycling and low volatility via experiments and simulations. Phys. Chem. Chem. Phys. *25*, 9320–9335. https://doi.org/10.1039/D2CP06089B.

14. Tundo, P., and Aricò, F. (2023). Reaction Pathways in Carbonates and Esters. ChemSusChem *16*, e202300748. https://doi.org/10.1002/cssc.202300748.

15. Shukla, K., and Srivastava, V.C. (2016). Diethyl Carbonate: Critical Review of Synthesis Routes, Catalysts Used and Engineering Aspects. RSC Adv. *6*, 32624–32645. https://doi.org/10.1039/C6RA02518H.

16. Zhou, Y., Fu, Z., Wang, S., Xiao, M., Han, D., and Meng, Y. (2016). Electrochemical Synthesis of Dimethyl Carbonate from CO_2 and Methanol over Carbonaceous Material Supported DBU in a Capacitor-like Cell Reactor. RSC Adv. *6*, 40010–40016. https://doi.org/10.1039/C6RA04150G.

17. Huang, S., Yan, B., Wang, S., and Ma, X. (2015). Recent Advances in Dialkyl Carbonates Synthesis and Applications. Chem. Soc. Rev. *44*, 3079–3116. https://doi.org/10.1039/C4CS00374H.

18. Jin Lee, H., Tung Nguyen, T., Vy Tran, A., Sik Kim, H., Suh, Y.-W., Baek, J., and Jin Kim, Y. (2023). Engineering pKa Value of 3° Amine for Enhanced Production of Dialkyl Carbonate via Se-Catalyzed Oxidative Carbonylation. J. Ind. Eng. Chem. *123*, 140–149. https://doi.org/10.1016/j.jiec.2023.03.030.

19. Cao, Y., Cheng, H., Ma, L., Liu, F., and Liu, Z. (2012). Research Progress in the Direct Synthesis of Dimethyl Carbonate from CO_2 and Methanol. Catal. Surv. Asia *16*, 138–147. https://doi.org/10.1007/s10563-012-9140-5.

20. Kongpanna, P., Pavarajarn, V., Gani, R., and Assabumrungrat, S. (2015). Techno-Economic Evaluation of Different CO_2-Based Processes for Dimethyl Carbonate Production. Chem. Eng. Res. Des. *93*, 496–510. https://doi.org/10.1016/j.cherd.2014.07.013.

21. Tomishige, K., Sakaihori, T., Sakai, S.i., and Fujimoto, K. (1999). Dimethyl Carbonate Synthesis by Oxidative Carbonylation on Activated Carbon Supported $CuCl_2$ Catalysts: Catalytic Properties and Structural Change. Appl. Catal. Gen. *181*, 95–102. https://doi.org/10.1016/S0926-860X(98)00386-X.

22. Matsuzaki, T., and Nakamura, A. (1997). Dimethyl Carbonate Synthesis and Other Oxidative Reactions Using Alkyl Nitrites. Catal. Surv. Asia. March *1997*, 77–88.

23. Dabral, S., and Schaub, T. (2019). The Use of Carbon Dioxide (CO_2) as a Building Block in Organic Synthesis from an Industrial Perspective. Adv. Synth. Catal. *361*, 223–246. https://doi.org/10.1002/adsc.201801215.

24. Omae, I. (2012). Recent Developments in Carbon Dioxide Utilization for the Production of Organic Chemicals. Coord. Chem. Rev. *256*, 1384–1405. https://doi.org/10.1016/j.ccr.2012.03.017.

25. Dibenedetto, A., and Angelini, A. (2014). Synthesis of Organic Carbonates. In Advances in Inorganic Chemistry, *66*Advances in Inorganic Chemistry (Elsevier), pp. 25–81. https://doi.org/10.1016/B978-0-12-420221-4.00002-0.

26. Chaban, V.V., Santos, L.M.d., and Einloft, S. (2024). Sodium fluoride enables room-temperature synthesis of dimethyl carbonate. J. Mol. Liq. *399*, 124417. https://doi.org/10.1016/j.molliq.2024.124417.

27. Chaban, V.V., Andreeva, N.A., Moreira dos Santos, L., and Einloft, S. (2024). Sodium chloride catalyzes valorization of carbon dioxide into dimethyl carbonate. J. Mol. Liq. *394*, 123743. https://doi.org/10.1016/j.molliq.2023.123743.

28. Chaban, V.V. (2023). Exothermic barrier-free carboxylation of alkali methylates. The highest-yield synthesis of dialkyl carbonates out of alcohols and carbon dioxide rationalized and reformulated through quantum-chemical simulations. J. Mol. Liq. *391*, 123244. https://doi.org/10.1016/j.molliq.2023.123244.

29. Jorapur, Y.R., and Chi, D.Y. (2005). Synthesis of Symmetrical Organic Carbonates via Significantly Enhanced Alkylation of Metal Carbonates with Alkyl Halides/Sulfonates in Ionic Liquid. J. Org. Chem. *70*, 10774–10777. https://doi.org/10.1021/jo051722h.

30. Verdecchia, M., Feroci, M., Palombi, L., and Rossi, L. (2002). A Safe and Mild Synthesis of Organic Carbonates from Alkyl Halides and Tetrabutylammonium Alkyl Carbonates. J. Org. Chem. *67*, 8287–8289. https://doi.org/10.1021/jo0259461.

31. Bratt, M.O., and Taylor, P.C. (2003). Synthesis of Carbonates and Related Compounds from Carbon Dioxide via Methanesulfonyl Carbonates. J. Org. Chem. *68*, 5439–5444. https://doi.org/10.1021/jo026753g.

32. Heldebrant, D.J., Yonker, C.R., Jessop, P.G., and Phan, L. (2008). Organic Liquid CO_2 Capture Agents with High Gravimetric CO_2 Capacity. Energy Environ. Sci. *1*, 487–493. https://doi.org/10.1039/b809533g.

33. Heldebrant, D.J., Jessop, P.G., Thomas, C.A., Eckert, C.A., and Liotta, C.L. (2005). The Reaction of 1,8-Diazabicyclo[5.4.0]undec-7-Ene (DBU) with Carbon Dioxide. J. Org. Chem. *70*, 5335–5338. https://doi.org/10.1021/jo0503759.

34. Khokarale, S.G., and Mikkola, J.-P. (2019). Metal Free Synthesis of Ethylene and Propylene Carbonate from Alkylene Halohydrin and CO_2 at Room Temperature. RSC Adv. *9*, 34023–34031. https://doi.org/10.1039/C9RA06765E.

35. Schottel, B.L., Chifotides, H.T., and Dunbar, K.R. (2008). Anion-π Interactions. Chem. Soc. Rev. *37*, 68–83. https://doi.org/10.1039/B614208G.

36. Luo, N., Ao, Y.F., Wang, D.X., and Wang, Q.Q. (2022). Putting Anion-π Interactions at Work for Catalysis. Chem. Eur J. *28*, e202103303. https://doi.org/10.1002/chem.202103303.

37. Harder, S., Streitwieser, A., Petty, J.T., and von Schleyer, P. (1995). Ion Pair SN2 Reactions. Theoretical Study of Inversion and Retention Mechanisms. J. Am. Chem. Soc. *117*, 3253–3259. https://doi.org/10.1021/ja00116a029.

38. Streitwieser, A., Choy, G.S.-C., and Abu-Hasanayn, F. (1997). Theoretical Study of Ion Pair S_N2 Reactions: Ethyl vs Methyl Reactivities and Extension to Higher Alkyls. J. Am. Chem. Soc. *119*, 5013–5019. https://doi.org/10.1021/ja961673d.

39. Ebrahimi, A., Habibi, M., and Amirmijani, A. (2007). The Study of Counterion Effect on the Reactivity of Nucleophiles in Some S_N2 Reactions in Gas Phase and Solvent Media. J. Mol. Struct. Theochem *809*, 115–124. https://doi.org/10.1016/j.theochem.2007.01.037.

40. Hamlin, T.A., Swart, M., and Bickelhaupt, F.M. (2018). Nucleophilic Substitution (S_N2): Dependence on Nucleophile, Leaving Group, Central Atom, Substituents, and Solvent. ChemPhysChem *19*, 1315–1330. https://doi.org/10.1002/cphc.201701363.

41. Fritz-Langhals, E. (2022). Unique Superbase TBD (1,5,7-Triazabicyclo[4.4.0]dec-5-ene): From Catalytic Activity and One-Pot Synthesis to Broader Application in Industrial Chemistry. Org. Process Res. Dev. *26*, 3015–3023. https://doi.org/10.1021/acs.oprd.2c00248.

42. Fu, X., and Tan, C.-H. (2011). Mechanistic Considerations of Guanidine-Catalyzed Reactions. Chem. Commun. *47*, 8210–8222. https://doi.org/10.1039/c0cc03691a.

43. Anderson, L.A., and Franz, A.K. (2012). Real-Time Monitoring of Transesterification by ^{1}H NMR Spectroscopy: Catalyst Comparison and Improved Calculation for Biodiesel Conversion. Energy Fuels *26*, 6404–6410. https://doi.org/10.1021/ef301035s.

44. Trapasso, G., Salaris, C., Reich, M., Logunova, E., Salata, C., Kümmerer, K., Figoli, A., and Aricò, F. (2022). A scale-up procedure to dialkyl carbonates; evaluation of their properties, biodegradability, and toxicity. Sustain. Chem. Pharm. *26*, 100639. https://doi.org/10.1016/j.scp.2022.100639.

45. Weiberth, F.J., Yu, Y., Subotkowski, W., and Pemberton, C. (2012). Demonstration on Pilot-Plant Scale of the Utility of 1,5,7-Triazabicyclo [4.4.0]dec-5-ene (TBD) as a Catalyst in the Efficient Amidation of an Unactivated Methyl Ester. Org. Process Res. Dev. *16*, 1967–1969. https://doi.org/10.1021/op300210j.

46. Sabot, C., Kumar, K.A., Meunier, S., and Mioskowski, C. (2007). A Convenient Aminolysis of Esters Catalyzed by 1,5,7-triazabicyclo[4.4.0]dec-5-ene (TBD) under Solvent-Free Conditions. Tetrahedron Lett. *48*, 3863–3866. https://doi.org/10.1016/j.tetlet.2007.03.146.

47. Vigante, B., Rucins, M., Plotniece, A., Pajuste, K., Luntena, I., Cekavicus, B., Bisenieks, E.,

Smits, R., Duburs, G., and Sobolev, A. (2015). Direct Aminolysis of Ethoxycarbonylmethyl 1,4-Dihydropyridine-3-Carboxylates. Molecules *20*, 20341–20354. https://doi.org/10.3390/molecules201119697.

48. Hickey, J.L., and Lin, S. (2020). One-pot Peptide Cleavage and Macrocyclization through Direct Amidation Using Triazabicyclodecene. Pept. Sci. *112* (4), e24161. https://doi.org/10.1002/pep2.24161.

49. Van Guyse, J.F.R., Verjans, J., Vandewalle, S., De Bruycker, K., Du Prez, F.E., and Hoogenboom, R. (2019). Full and Partial Amidation of Poly(methyl Acrylate) as Basis for Functional Polyacrylamide (Co)Polymers. Macromolecules *52*, 5102–5109. https://doi.org/10.1021/acs.macromol.9b00399.

50. Hoogenboom, R., and Van Guyse, J. (2022). Amidation of Polymers Containing Ester Side Chains Using Functionalized Amines. US11332554B2. https://patents.google.com/patent/US11332554B2/en.

51. Mutlu, H., and Meier, M.A.R. (2009). Unsaturated PA X,20 from Renewable Resources via Metathesis and Catalytic Amidation. Macromol. Chem. Phys. *210*, 1019–1025. https://doi.org/10.1002/macp.200900045.

52. Guo, W., Gómez, J.E., Martínez-Rodríguez, L., Bandeira, N.A.G., Bo, C., and Kleij, A.W. (2017). Metal-Free Synthesis of *N*-Aryl Amides Using Organocatalytic Ring-Opening Aminolysis of Lactones. ChemSusChem *10*, 1969–1975. https://doi.org/10.1002/cssc.201700415.

53. Rankic, D.A., Stiff, C.M., am Ende, C.W., and Humphrey, J.M. (2017). Protocol for the Direct Conversion of Lactones to Lactams Mediated by 1,5,7-Triazabicyclo[4.4.0]dec-5-ene: Synthesis of Pyridopyrazine-1,6-diones. J. Org. Chem. *82*, 12791–12797. https://doi.org/10.1021/acs.joc.7b02079.

54. Horváth, A. (1996). Catalysis and Regioselectivity in the Michael Addition of Azoles. Kinetic vs. Thermodynamic Control. Tetrahedron Lett. *37*, 4423–4426. https://doi.org/10.1016/0040-4039(96)00845-3.

55. Ghobril, C., Sabot, C., Mioskowski, C., and Baati, R. (2008). TBD-Catalyzed Direct 5- and 6-*Enolexo* Aldolization of Ketoaldehydes. Eur. J. Org. Chem. *2008*, 4104–4108. https://doi.org/10.1002/ejoc.200800539.

56. Kiesewetter, M.K., Scholten, M.D., Kirn, N., Weber, R.L., Hedrick, J.L., and Waymouth, R.M. (2009). Cyclic Guanidine Organic Catalysts: What Is Magic About Triazabicyclodecene? J. Org. Chem. *74*, 9490–9496. https://doi.org/10.1021/jo902369g.

57. Baidya, M., and Mayr, H. (2008). Nucleophilicities and Carbon Basicities of DBU and DBN. Chem. Commun. *15*, 1792–1794. https://doi.org/10.1039/b801811a.

58. Munshi, P., Main, A.D., Linehan, J.C., Tai, C.-C., and Jessop, P.G. (2002). Hydrogenation of Carbon Dioxide Catalyzed by Ruthenium Trimethylphosphine Complexes: The Accelerating Effect of Certain Alcohols and Amines. J. Am. Chem. Soc. *124*, 7963–7971. https://doi.org/10.1021/ja0167856.

59. Xia, Y., Shen, J., Alamri, H., Hadjichristidis, N., Zhao, J., Wang, Y., and Zhang, G. (2017). Revealing the Cytotoxicity of Residues of Phosphazene Catalysts Used for the Synthesis of Poly(ethylene Oxide). Biomacromolecules *18*, 3233–3237. https://doi.org/10.1021/acs.biomac.7b00891.

60. Khalil, A., Saba, S., Ribault, C., Vlach, M., Loyer, P., Coulembier, O., and Cammas-Marion, S. (2020). Synthesis of Poly(Dimethylmalic Acid) Homo- and Copolymers to Produce Biodegradable Nanoparticles for Drug Delivery: Cell Uptake and Biocompatibility Evaluation in Human Heparg Hepatoma Cells. Polymers *12*, 1705. https://doi.org/10.3390/polym12081705.

61. Mathias, P.M., Afshar, K., Zheng, F., Bearden, M.D., Freeman, C.J., Andrea, T., Koech, P.K., Kutnyakov, I., Zwoster, A., Smith, A.R., et al. (2013). Improving the Regeneration of CO_2-Binding Organic Liquids with a Polarity Change. Energy Environ. Sci. *6*, 2233. https://doi.org/10.1039/c3ee41016a.

62. Gui, X., Tang, Z., and Fei, W. (2011). Solubility of CO_2 in Alcohols, Glycols, Ethers, and Ketones at High Pressures from (288.15 to 318.15. J. Chem. Eng. Data *56*, 2420–2429. https://doi.org/10.1021/je101344v.

63. Phan, L., Chiu, D., Heldebrant, D.J., Huttenhower, H., John, E., Li, X., Pollet, P., Wang, R., Eckert, C.A., Liotta, C.L., and Jessop, P.G. (2008). Switchable Solvents Consisting of Amidine/Alcohol or Guanidine/Alcohol Mixtures. Ind. Eng. Chem. Res. *47*, 539–545. https://doi.org/10.1021/ie070552r.

64. Sakai, S., Kobayashi, Y., and Ishii, Y. (1971). Reaction of dialkyltin dialkoxides with carbon disulfide at higher temperature. Preparation of orthocarbonates. J. Org. Chem. *36*, 1176–1180. https://doi.org/10.1021/jo00808a002.

65. Pérez, E.R., Santos, R.H.A., Gambardella, M.T.P., de Macedo, L.G.M., Rodrigues-Filho, U.P., Launay, J.-C., and Franco, D.W. (2004). Activation of Carbon Dioxide by Bicyclic Amidines. J. Org. Chem. *69*, 8005–8011. https://doi.org/10.1021/jo049243q.

66. Villiers, C., Dognon, J.-P., Pollet, R., Thuéry, P., and Ephritikhine, M. (2010). An Isolated CO_2 Adduct of a Nitrogen Base: Crystal and Electronic Structures. Angew. Chem. Int. Ed. *49*, 3465–3468. https://doi.org/10.1002/anie.201001035.

67. Winstein, S., Clippinger, E., Fainberg, A.H., Heck, R., and Robinson, G.C. (1956). Salt Effects and Ion Pairs in Solvolysis and Related Reactions. III.[1] Common Ion Rate Depression and Exchange of Anions during Acetolysis[2,3]. J. Am. Chem. Soc. *78*, 328–335. https://doi.org/10.1021/ja01583a022.

68. Contreras-García, J., Johnson, E.R., Keinan, S., Chaudret, R., Piquemal, J.-P., Beratan, D.N., and Yang, W. (2011). NCIPLOT: A Program for Plotting Noncovalent Interaction Regions. J. Chem. Theory Comput. *7*, 625–632. https://doi.org/10.1021/ct100641a.

69. Alfassi, Z.B., Huie, R.E., Milman, B.L., and Neta, P. (2003). Electrospray Ionization Mass Spectrometry of Ionic Liquids and Determination of their Solubility in Water. Anal. Bioanal. Chem. *377*, 159–164. https://doi.org/10.1007/s00216-003-2033-8.

70. Wang, P., Zakeeruddin, S., Grätzel, M., Kantlehner, W., Mezger, J., Stoyanov, E.V., and Scherr, O. (2004). Novel Room Temperature Ionic Liquids of Hexaalkyl Substituted Guanidinium Salts for Dye-sensitized Solar Cells. Appl. Phys. A *79*, 73–77. https://doi.org/10.1007/s00339-003-2505-x.

71. Yi, C., Luo, J., Meloni, S., Boziki, A., Ashari-Astani, N., Grätzel, C., Zakeeruddin, S.M., Röthlisberger, U., and Grätzel, M. (2016). Entropic Stabilization of Mixed A-cation ABX_3 Metal Halide Perovskites for High Performance Perovskite Solar Cells. Energy Environ. Sci. *9*, 656–662. https://doi.org/10.1039/C5EE03255E.

72. Mesias-Salazar, A., Rojas, R.S., Carrillo-Hermosilla, F., Martinez, J., Antinolo, A., Trofymchuk, O.S., Nachtigall, F.M., Santos, L.S., and Daniliuc, C.G. (2023). Guanidinium Iodide Salts as Single Component Catalyst in CO_2 to Epoxide Fixation. New J. Chem. *48*, 105–111. https://doi.org/10.1039/D3NJ03959E.

73. Mosmann, T. (1983). Rapid colorimetric assay for cellular growth and survival: application to proliferation and cytotoxicity assays. J. Immunol. Methods *65*, 55–63. https://doi.org/10.1016/0022-1759(83)90303-4.

74. Kanwar, J.R., and Kanwar, R.K. (2009). Gut Health Immunomodulatory and Anti-Inflammatory Functions of Gut Enzyme Digested High Protein Micro-Nutrient Dietary Supplement-Enprocal. BMC Immunol. *10*, 7. https://doi.org/10.1186/1471-2172-10-7.

75. Frisch, M.J., Trucks, G.W., Schlegel, H.B., Scuseria, G.E., Robb, M.A., Cheeseman, J.R., Scalmani, G., Barone, V., Petersson, G.A., Nakatsuji, H., et al. (2016). Gaussian 16, Revision C.01 (Gaussian, Inc.).

76. Becke, A.D. (1993). Density-functional Thermochemistry. III. The Role of Exact Exchange. J. Chem. Phys. *98*, 5648–5652. https://doi.org/10.1063/1.464913.

77. Lee, C., Yang, W., and Parr, R.G. (1988). Development of the Colle-Salvetti Correlation-Energy Formula into a Functional of the Electron Density. Phys. Rev. B *37*, 785–789. https://doi.org/10.1103/PhysRevB.37.785.

78. Andrae, D., H-u-ermann, U., Dolg, M., Stoll, H., and Preu-, H. (1990). Energy-Adjustedab Initio Pseudopotentials for the Second and Third Row Transition Elements. Theor. Chim. Acta *77*, 123–141. https://doi.org/10.1007/BF01114537.

79. Clark, T., Chandrasekhar, J., Spitznagel, G.W., and Schleyer, P.V.R. (1983). Efficient Diffuse Function-Augmented Basis Sets for Anion Calculations. III. The 3-21+G Basis Set for First-Row Elements, Li–F. J. Comput. Chem. *4*, 294–301. https://doi.org/10.1002/jcc.540040303.

80. Krishnan, R., Binkley, J.S., Seeger, R., and Pople, J.A. (1980). Self-consistent Molecular Orbital Methods. XX. A Basis Set for Correlated Wave Functions. J. Chem. Phys. *72*, 650–654. https://doi.org/10.1063/1.438955.

81. Cossi, M., Rega, N., Scalmani, G., and Barone, V. (2003). Energies, Structures, and Electronic Properties of Molecules in Solution with the

C-PCM Solvation Model. J. Comput. Chem. *24*, 669–681. https://doi.org/10.1002/jcc.10189.

82. Grimme, S., Antony, J., Ehrlich, S., and Krieg, H. (2010). A Consistent and Accurate Ab Initio Parametrization of Density Functional Dispersion Correction (DFT-D) for the 94 Elements H-Pu. J. Chem. Phys. *132*, 154104. https://doi.org/10.1063/1.3382344.

83. Grimme, S., Ehrlich, S., and Goerigk, L. (2011). Effect of the Damping Function in Dispersion Corrected Density Functional Theory. J. Comput. Chem. *32*, 1456–1465. https://doi.org/10.1002/jcc.21759.

84. Humphrey, W., Dalke, A., and Schulten, K. (1996). VMD: Visual Molecular Dynamics. J. Mol. Graph. *14*, 33–38. https://doi.org/10.1016/0263-7855(96)00018-5.

85. Legault, C.Y. (2009). CYL*view*, Version 1.0b; Universitéde Sherbrooke. http://www.cylview.org.